

Reaction  $C^{12}(d,n)N^{13}\dagger$ A. ELWYN,\* J. V. KANE, S. OFER,† AND D. H. WILKINSON§  
*Brookhaven National Laboratory, Upton, New York*

(Received July 30, 1959)

The reaction  $C^{12}(d,n)N^{13}$  has  $Q = -0.28$  Mev and so is expected to show strong direct interaction effects even at low energies of the bombarding deuterons. We have made an extensive study of this reaction at 14 values of the deuteron energy between  $E_d = 1.45$  Mev and  $E_d = 2.95$  Mev. At each deuteron energy the differential cross section was measured at about 20 angles between  $0^\circ$  and  $165^\circ$ . Neutron time-of-flight techniques were used and each point on each angular distribution represents the detection of at least  $10^3$  neutrons. Direct interaction effects are seen at all bombarding energies in the backward as well as in the forward hemisphere. The differential cross section at  $0^\circ$  shows very pronounced "resonance" structure but this largely disappears in the integrated cross section and is due chiefly to interference between the direct interaction term and the probably quite small compound nucleus contribution. A rough method for eliminating the interference terms between the two mechanisms in the differential cross section is proposed and applied. The resultant "purified" angular distribution is remarkably close, in the forward hemisphere, to that predicted by simple stripping theory. A backward maximum, much lower than the forward peak, is also present but not accounted for.

## INTRODUCTION

IT is well known that the angular distributions of the outgoing particles in  $(d,p)$  and  $(d,n)$  reactions leading to definite final states show strong peaking in the forward hemisphere for moderate deuteron bombarding energies. Butler and others<sup>1</sup> have shown how to interpret these distributions in terms of the angular momentum  $l$ , carried into the target nucleus by the captured particle. The original formulations of the theory made drastic approximations and, even in the most favorable cases, were not able to explain the experimental shapes in all their details. Modifications which have taken into account the Coulomb and nuclear interactions of the particles involved have improved the fit with experiment especially in the angular regions away from the primary maximum in the distribution. At lower incident energies the theoretical patterns are especially sensitive to the particular model chosen for the nuclear interaction.<sup>2</sup>

At the present time there is no consistent method of including the contribution to the differential cross section from compound nucleus formation. Such contributions exist even at incident energies above the Coulomb barrier of the target nucleus. As the incident energy is made equal to or less than the barrier height, compound nucleus effects tend to become more important, and in many cases may dominate over the stripping contributions, smearing out the strong asymmetries in the angular distributions. The initial- and final-state interactions, both nuclear and Coulomb, however, have a similar effect and it is impossible to

assess the relative contribution of compound nucleus formation merely by inspection of the angular distribution. Even if the pure distributions (stripping and compound nucleus) were well-known, interference between them would invalidate any simple subtraction procedure at one bombarding energy. There have been various attempts, all more-or-less unsatisfactory, to assess the importance of compound nuclear effects in deuteron induced reactions at low energies.<sup>3,4</sup>

It has been pointed out recently<sup>5</sup> that  $(d,p)$  and  $(d,n)$  reactions initiated by low-energy deuterons, leading to residual nuclear states of low  $Q$ -value ( $\pm 2$  Mev), may actually show stripping patterns superior to those seen at higher energies and higher  $Q$ -values. Qualitatively, a low  $Q$ -value reaction means low binding energy of the captured nucleon in the residual nucleus. Thus, the ingoing particle need not be closer than a few fermis ( $1 \text{ fermi} = 10^{-13} \text{ cm}$ ) to the nuclear surface when captured. Furthermore, the outgoing particle needs only a small momentum transfer (owing to low incident deuteron energy and low  $Q$ -value) which it can get from the internal deuteron wave function even though the neutron and proton may be widely separated at the time of stripping. The outgoing particle, therefore, never gets close to the nuclear surface and need never feel the effects of the nuclear interaction. Thus we satisfy one of the basic approximations of the primitive stripping theories. This picture can explain the well-developed stripping patterns which are observed at low deuteron energies. The effects mentioned above should be more marked for  $(d,p)$  than for  $(d,n)$  reactions at low energy in all but the lightest nuclei owing to Coulomb barrier effects.<sup>5</sup>

† Work performed under the auspices of the U. S. Atomic Energy Commission.

\* Permanent address: Argonne National Laboratory, Lemont, Illinois.

‡ On leave from The Hebrew University, Jerusalem, Israel.

§ Permanent address: Clarendon Laboratory, Oxford, England.

<sup>1</sup> S. T. Butler, Proc. Roy. Soc. (London) **A208**, 559 (1952); Bhatia, Huang, Huby, and Newins, Phil. Mag. **43**, 485 (1952); P. B. Daitch and J. B. French Phys. Rev. **87**, 900 (1952).

<sup>2</sup> W. Tobocman and M. H. Kalos, Phys. Rev. **97**, 132 (1955).

<sup>3</sup> See, for example: McEllistrem, Jones, Chiba, Douglas, Herring, and Silverstein, Phys. Rev. **104**, 1008 (1956); M. T. McEllistrem, Phys. Rev. **111**, 596 (1958); J. B. Marion and G. Weber, Phys. Rev. **102**, 1355 (1956); G. C. Phillips, Phys. Rev. **80**, 164 (1950).

<sup>4</sup> Bonner, Eisinger, Kraus, and Marion, Phys. Rev. **101**, 209 (1956).

<sup>5</sup> D. H. Wilkinson, Phil. Mag. **3**, 1185 (1958).

The  $C^{12}(d,n)N^{13}$  ground-state reaction has a  $Q$ -value of  $-0.281$  Mev,<sup>6</sup> so that for low deuteron energies, according to the above discussion, well-developed stripping patterns might be expected to result. This paper presents the results of a study of the angular distributions of the neutrons in this reaction over a range of incident energies from 1.45 to 2.95 Mev in an attempt to study the importance to the cross section of stripping and compound nuclear contributions, and to observe the interference effects between the two mechanisms.

In addition to this particular consideration the effects of direct interactions of other types (e.g., heavy-particle stripping and surface reflection) formed a secondary objective of this work because it is well known that severe disagreement exists between experiment and usual stripping theory at backward angles.

Peaks apparently corresponding to levels in the compound nucleus  $N^{14}$  have been observed in the  $C^{12}+d$  reactions in the energy range 700 keV to 5 Mev<sup>3,4</sup> and in the  $B^{10}+\alpha$  reactions<sup>6</sup> at the same excitation in  $N^{14}$ . Thus, compound nucleus formation is known to occur in deuteron-induced reactions on carbon. The ground-state (g.s.) spin and parity of  $N^{13}$  is  $\frac{1}{2}^-$ , and since the spin-parity assignment of  $C^{12}$  is  $0+$ , angular momentum conservation would predict that, if the reaction proceeded predominantly by stripping, the angular momentum of the captured proton would be  $l_p=1$ . The angular distributions of the outgoing neutrons in the  $C^{12}(d,n)N^{13}$  (g.s.) reaction at various energies<sup>4,7</sup> have shown that such is the case, and thus that stripping does indeed occur.

In order to study the interference between compound nucleus formation and direct interaction, one takes advantage of the nature of these processes by realizing that effects contributed by the compound state are very sensitive to the energy of excitation (and hence to the bombarding energy), whereas those contributed by direct interaction processes should be relatively slowly varying functions of the bombarding energy. On this basis it is desirable to make measurements of the angular distribution at energy intervals whose spacing is small compared with the observed level spacings. A corollary of these remarks is that, where two such mechanisms are competing, an excitation function taken at a single angle, will not, in general, give a reliable indication of their relative intensities. Further difficulties arise in the location of energy levels in the compound system by observation of maxima in the differential cross section at one angle. This procedure may give rise to apparent differences in energy of identical levels which are observed through different reactions. For example, the differential cross-section maxima observed, say, in  $C^{12}(d,p)C^{13}$ ,

<sup>6</sup> F. Ajzenberg and T. Lauritsen, *Revs. Modern Phys.* **27**, 77 (1955).

<sup>7</sup> Middleton *et al.*, *Proc. Phys. Soc. (London)* **A66**, 95 (1953); Benenson, Jones, and McEllistrem, *Phys. Rev.* **101**, 308 (1956).

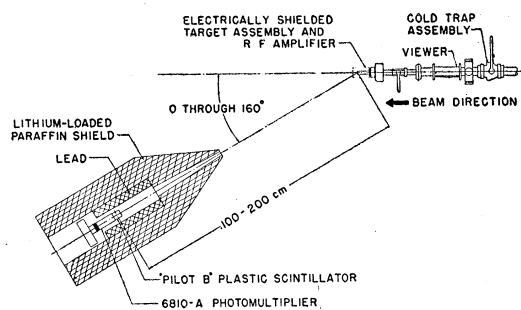


FIG. 1. Target and detector arrangement employed in the measurement of the reaction  $C^{12}(d,n)N^{13}$ .

$C^{12}(d,n)N^{13}$ , and  $B^{10}(\alpha,p)C^{13}$  may appear to correspond to different sets of "levels" in  $N^{14}$ .<sup>8</sup>

The present study of a  $(d,n)$  reaction, in which the angular distributions are examined over a wide range of incident energies, is made possible because of the extension and improvement of time-of-flight spectroscopy to the fast neutron region. The use of millimicrosecond pulsing techniques in conjunction with Van de Graaff accelerators<sup>9</sup> has already shown the broad utility of the method for fast-neutron spectroscopy.

#### EXPERIMENTAL CONSIDERATIONS

The Brookhaven National Laboratory Van de Graaff accelerator has been fitted with a pair of electrostatic deflection plates in order to produce pulses of charged particles. These plates have been placed at a point directly after the ions emerge from the probe and preaccelerator electrodes in the high voltage terminal of the machine. The technique and apparatus have been described by Turner and Bloom.<sup>10</sup> By applying an rf voltage of 7.6 Mc/sec to the plates, and by use of two pairs of electrostatic refractor plates, it is possible in the present setup to accelerate bursts of deuterons of 2 to 3 millimicrosecond ( $m\mu$ sec) duration so that one burst per period of the rf voltage (about 130  $m\mu$ sec) with an average current of about 0.2  $\mu$ a can be made to impinge upon targets placed at the end of a suitable length of beam pipe.

Figure 1 presents a schematic diagram of the experimental setup. A thin carbon target was prepared by smoking a clean tantalum blank in a benzene flame. The thickness of the target was measured by weighing and determined to be approximately 0.3 milligram/cm<sup>2</sup>. Neutrons from the  $(d,n)$  reaction in the target pass down a known flight path inside a suitable shield,<sup>11</sup> which could be pivoted from a point beneath the

<sup>8</sup> See Figs. 8 and 9 of McEllistrem, Jones, Chiba, Douglas, Herring, and Silverstein, *Phys. Rev.* **104**, 1008 (1956).

<sup>9</sup> L. Cranberg and J. S. Levin, *Phys. Rev.* **103**, 343 (1956).

<sup>10</sup> C. M. Turner and S. D. Bloom, *Rev. Sci. Instr.* **29**, 480 (1958). The actual timing system employed in the present experiment has been modified from that described in this reference (see text).

<sup>11</sup> The design of the shield is described in Landon, Elwyn, Glasoe, and Oleksa, *Phys. Rev.* **112**, 1192 (1958).

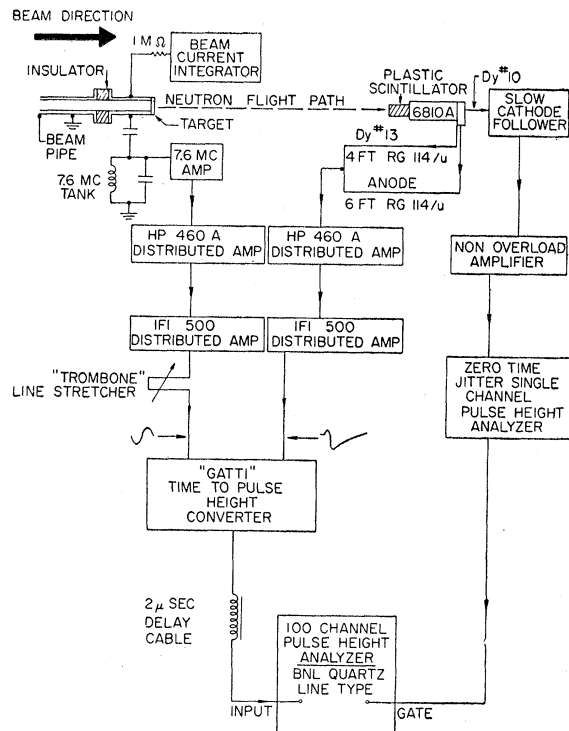


FIG. 2. Block diagram of millimicrosecond timing apparatus.

target, and were detected by a  $1\frac{3}{4}$ -in. diameter by 2-in. long plastic scintillator<sup>12</sup> mounted on an RCA type 6810A photomultiplier tube. In these measurements the flight path is about 100 cm. The timing of the neutrons is accomplished by referring a "fast" signal from the anode and dynode No. 13 of the phototube to a beam phase signal obtained electrically when the deuterons enter the target,<sup>13</sup> in a special time-to-pulse height converter. The converter is based on an rf vernier technique<sup>14</sup> suitably modified<sup>13</sup> for the present purpose. The output of the converter was displayed on a 100-channel analyzer which was gated by a "slow" signal from a pulse-height discriminator. This signal was obtained from dynode No. 10 of the phototube and provided a means of pulse-height selection of the signals displayed on the 100-channel analyzer. The discriminator bias on the slow side was suitably adjusted so that neutrons corresponding to  $N^{13}$  in its ground state were detected with close to 100% electronic efficiency for the range of deuteron bombarding energies used.

For neutron energies above  $\sim 1.5$  Mev no difficulty was experienced with discriminator settings which were set at a few percent of the maximum pulse height observed for neutrons of this energy. At neutron

<sup>12</sup> Type Pilot B, Pilot Chemical Corporation, Boston, Massachusetts.

<sup>13</sup> J. V. Kane, Rev. Sci. Instr. (to be published).

<sup>14</sup> C. Cottini and E. Gatti, Nuovo cimento 4, 1550 (1956); R. L. Chase and W. A. Higinbotham, Rev. Sci. Instr. 28, 448 (1957).

energies below this value, however, too high a discriminator setting could result in an appreciably reduced neutron efficiency and too low a discriminator setting could produce an undesirably large continuous background. This effect was investigated by plotting the neutron group counts with background subtracted as a function of discriminator setting. It was possible (with the exception of the backward angles at the lowest bombarding energy) to set the discriminator low enough so that for most of the data presented herein, at least, 98% of the neutrons detected in the plastic scintillator were registered properly. At  $E_d = 1.45$  Mev and  $\theta = 150^\circ$  this effect did not exceed 5%. A block diagram of the electronic circuits employed is shown in Fig. 2.

A typical time-of-flight spectrum is shown in Fig. 3. The ordinate gives the total number of counts for a given number of coulombs of integrated beam current; the abscissa is channel number on the 100-channel

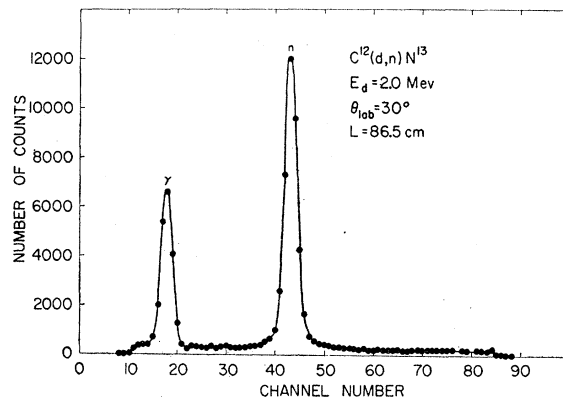


FIG. 3. Typical time-of-flight spectrum obtained with the apparatus described in this paper. (Note: Time increases from left to right; time zero is inferred from the position of the gamma-ray peak; see text).

display. In this curve time runs from left to right, and, as can be seen, about 75 channels correspond to the period of the rf voltage (about 130  $\mu$ sec). Since the detector is sensitive to gamma rays as well as neutrons, a peak appears on the time scale corresponding to  $\gamma$ -rays arising in the target. For a flight path of about 100 cm these arrive at the detector about 3.3  $\mu$ sec after the deuterons hit the target. The peak marked  $n$  corresponds to the neutrons obtained in the  $C^{12}(d,n)N^{13}$  (g.s.) reaction. No other neutron group is seen as the incident energy was too low to excite the first excited state in  $N^{13}$ . The flat portion of the spectrum represents a background due to radioactivity in the target, radioactivity in the room, and other sources of time uncorrelated radiation. The linearity of the time display was periodically checked throughout the experiment by use of a radioactive source as a source of random pulses and an rf generator; the time spectrum so obtained was flat within  $\pm 10\%$ .

Deuteron bombarding energies quoted in this report are those energies as read on a generating voltmeter. The actual bombarding energies were possibly higher by about 40 keV if the meter was accurate because of the additional energy given to the particles by the focusing electrodes in the high-voltage terminal. However, because of possible uncertainties of  $\pm 20$  keV in the voltmeter readings, and because of energy losses of the deuterons in the carbon target, it was felt that the energies reported represent reasonably correct values for the energies of the deuterons producing the reaction.

The yield curve of neutrons in the  $C^{12}(d,n)N^{13}$  reaction leading to the  $N^{13}$  ground state was obtained with the shielded detector set at an angle of  $0^\circ$  to the incident deuteron beam. The bombarding energy was varied in 25-keV steps from 1.40 to 3.125 MeV, and a complete time spectrum obtained at each energy; each run was normalized to the same number of coulombs.

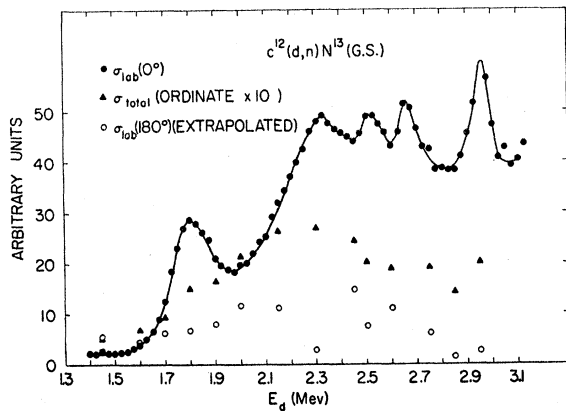


FIG. 4. Total cross-section points (triangles) and  $0^\circ$  yield curve of the reaction  $C^{12}(d,n)N^{13}$  as a function of deuteron bombarding energy.

The raw data consisting of the total number of counts in the neutron peaks minus appropriate backgrounds obtained from the flat portions of the spectra were corrected for dead time losses in the 100-channel analyzer (which were never greater than about 20%), buildup of carbon on the target, and for the efficiency of the plastic phosphor. This efficiency as a function of neutron energy was calculated approximately by a method described in the Appendix. Figure 4 shows the yield as a function of deuteron bombarding energy at  $0^\circ$  in the laboratory. No absolute cross sections are given. The curve is in good agreement with previous investigations.<sup>15</sup>

Angular distributions of the neutrons were obtained at deuteron bombarding energies of 1.45, 1.6, 1.7, 1.8, 1.9, 2.0, 2.15, 2.3, 2.45, 2.5, 2.6, 2.75, 2.85, and 2.95 MeV by pivoting the shielded detector underneath the

<sup>15</sup> N. Jarmie and J. D. Seagrave, Los Alamos Scientific Laboratory Report LA-2014, 1957 (unpublished); Bailey, Freier, and Williams, *Phys. Rev.* **73**, 274 (1948).

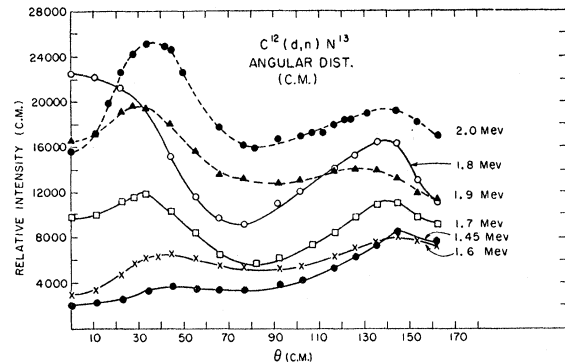


FIG. 5. Differential cross section of the reaction  $C^{12}(d,n)N^{13}$  in arbitrary units as a function of center-of-mass angle at bombarding energies indicated.

target, and obtaining a time spectrum at each of about 20 angles at each bombarding energy. In addition to the corrections mentioned above, it was necessary to correct the raw data for neutron absorption in the material around the target area, the amount of which differed from angle to angle. It was found that for the range of neutron energies covered, the total neutron loss for the materials involved varied by 15% or less.<sup>16</sup> Included in these corrections was the effect of a 3-mm aluminum absorber whose purpose was to absorb the  $N^{13}$  positrons emitted by the target. Using average total cross sections and measured amounts of the substances involved, approximate neutron transmissions were calculated at each angle. In order to check these results a measurement of the  $D(d,n)He^3$  cross section at a particular energy, using a  $Al_2O_3 \cdot X D_2O$  target, was compared to the known  $d$ - $D$  cross section<sup>17</sup> in the backward angles where the neutron absorption is greatest; thus, experimental neutron transmissions were obtained. Agreement between these measurements

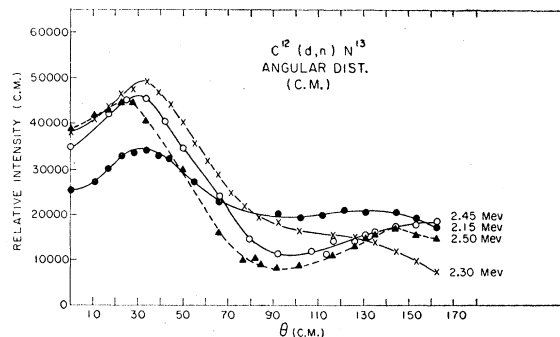


FIG. 6. Differential cross section of the reaction  $C^{12}(d,n)N^{13}$  in arbitrary units as a function of center-of-mass angle at bombarding energies indicated.

<sup>16</sup> *Neutron Cross Sections*, compiled by D. J. Hughes and R. Schwartz, Brookhaven National Laboratory Report BNL-325 (Superintendent of Documents, U. S. Government Printing Office, Washington, D. C., 1958), second edition.

<sup>17</sup> J. L. Fowler and J. E. Brolley, Jr., *Revs. Modern Phys.* **28**, 103 (1956).

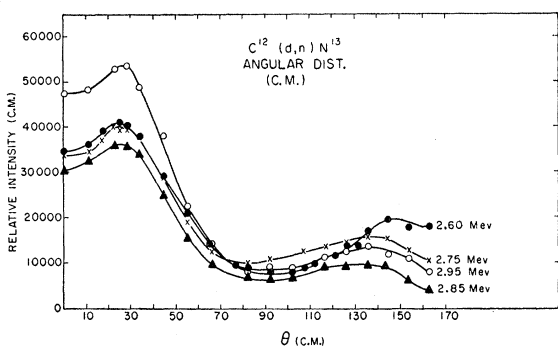


FIG. 7. Differential cross section of the reaction  $C^{12}(d,n)N^{13}$  in arbitrary units as a function of center-of-mass angle at bombarding energies indicated.

and the calculated transmissions were used to correct the data at each angle. Figures 5, 6, and 7 show the angular distributions in the center-of-mass system.<sup>18</sup>

Total cross sections in the  $C^{12}(d,n)N^{13}$  reaction were obtained at each bombarding energy for which an angular distribution was obtained by multiplying each point on the angular distribution in the laboratory system by  $\sin\theta$ , and integrating the resulting curve. These points are shown as the triangles in Fig. 4. Also included in Fig. 4 are points at  $180^\circ$  in the laboratory system obtained by extrapolating the angular distributions to the backward direction.

#### DISCUSSION

Each angular distribution was fitted by the elementary Butler theory formulation using the tables of

Lubitz<sup>19</sup> for a value of  $l_p=1$ . The "radius,"  $r$ , of this theory was treated as an adjustable parameter; the value chosen so that the peak of the theoretical distribution fits the experimental distributions. Figures 8-13 show the Butler fits to the angular distributions.

There is of course no merit in this quite arbitrary procedure other than the general demonstration that such fits can be forced for values of the effective stripping radius that are physically reasonable. It is, however, very remarkable that the experimental angular distributions so closely resemble the most primitive theoretical predictions. It is particularly noteworthy that the ratio of cross sections at the peak and at  $0^\circ$  should so closely tally with the simple prediction and the agreement as to the rate of fall of cross section beyond the peak towards  $90^\circ$  is also remarkable. At only one of our bombarding energies (1.80 Mev) does the forward peak not appear at an angle consistent with  $l_p=1$ . It is clear that although from the  $0^\circ$  excitation function (Fig. 4) resonances appear to be very important, yet in fact the course of the angular distribution is guided chiefly by direct interaction at all or almost all bombarding energies. The rapid variations of the  $0^\circ$  cross section are due chiefly to interference between the underlying direct interaction mechanism and the effects of individual levels, and we obviously cannot interpret their amplitude as a representation of the relative importance of compound nucleus formation. This is emphasized by comparing the integrated cross section with the  $0^\circ$  differential cross section (Fig. 4). As can be seen, the

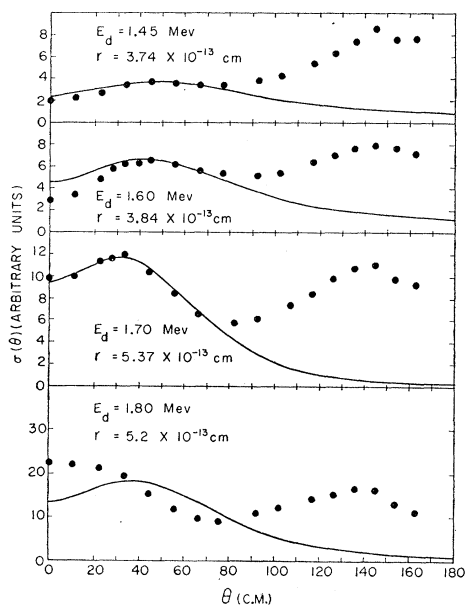


FIG. 8. Butler fit to differential cross section at 1.45, 1.60, 1.70, 1.80, Mev (see text).

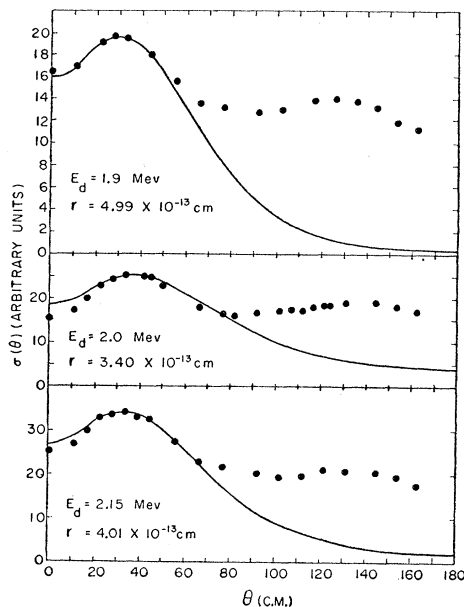


FIG. 9. Butler fit to differential cross section at 1.9, 2.0, 2.15 Mev.

<sup>18</sup> J. B. Marion and A. S. Ginzberg, Atomic Energy Commission Report NP-6241, 1957 (unpublished).

<sup>19</sup> C. R. Lubitz, Atomic Energy Commission Report AECU-3990, 1957 (unpublished).

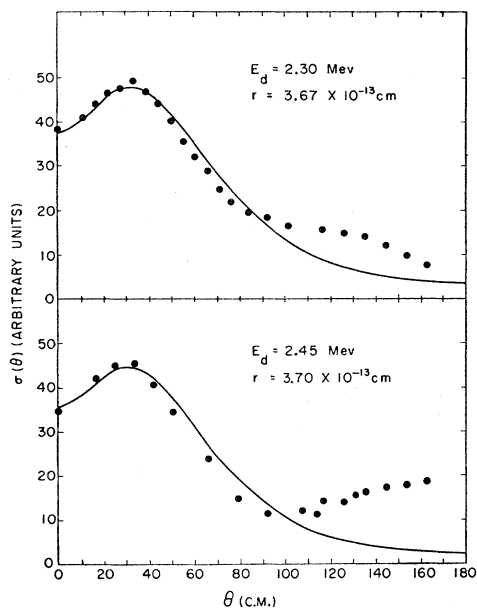


FIG. 10. Butler fit at 2.3 and 2.45 Mev.

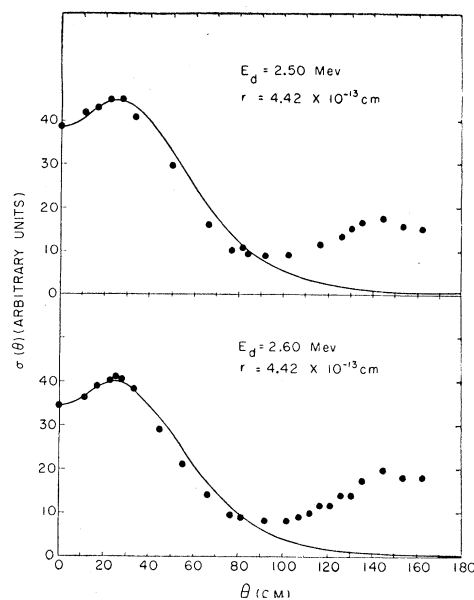


FIG. 11. Butler fit at 2.50 and 2.60 Mev.

integrated cross section is very different in its structure from the differential  $0^\circ$  cross section and shows none of the sharp and pronounced "resonances" though it is in the total cross section that compound nucleus effects must appear if they truly represent a major contribution to the reaction mechanism. A similarly interesting comparison is between the  $0^\circ$  and extrapolated  $180^\circ$  differential cross sections. It is seen that the correlation is poor and sometimes there is an anticorrelation. This is indeed what we should expect if the bulk of the "resonance" structure is due to interference effects between the two mechanisms. The clear conclusion of this study is that although such maxima and minima at a given angle indicate the presence of compound nucleus resonances whose spacing in excitation is of the order of the spacing of the structure in the  $0^\circ$  differential cross section,<sup>20</sup> we cannot say more than this and in particular cannot conclude that a resonance level exists at excitation corresponding to a maximum in the differential cross section taken at any arbitrarily chosen angle.

Equally persistent with the forward maximum, though not so well-marked, is the backward maximum at less than  $180^\circ$  seen at almost all bombarding energies (the two energies where it is not clear,  $E_d=2.30$  and  $2.45$  Mev, have strikingly different behavior near  $180^\circ$  and this is obviously another demonstration of the importance of interference effects). Since this backward peaking at a finite angle carries through the whole range of bombarding energy (Fig. 14), it must equally be a direct interaction phenomenon though

<sup>20</sup> The level spacing alternatively might be rather less than this and we see the result of interference with the fluctuations of the compound nucleus level density.

not one predicted by the simplest stripping model. This might emerge from a more refined calculation of ordinary stripping as a distorted wave effect. It might alternatively represent some additional direct interaction mechanism such as heavy-particle stripping.<sup>21</sup> This latter we should expect to be relatively unimportant here because of the very high binding energy (18.7 Mev) of a neutron in  $C^{12}$ . As a check we have plotted some of the observed cross sections as a function of the magnitude of the heavy-particle momentum transfer vector (Fig. 15). No correlation is observed between the backward peak and any single heavy-particle effective radius of stripping. It is concluded

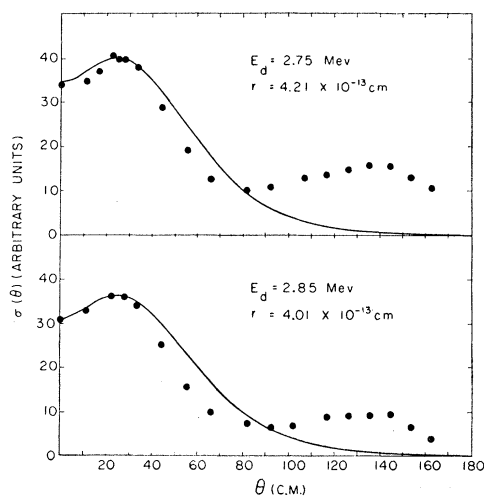


FIG. 12. Butler fit at 2.75 and 2.85 Mev.

<sup>21</sup> G. E. Owen and L. Madansky, Phys. Rev. **99**, 1608 (1955).

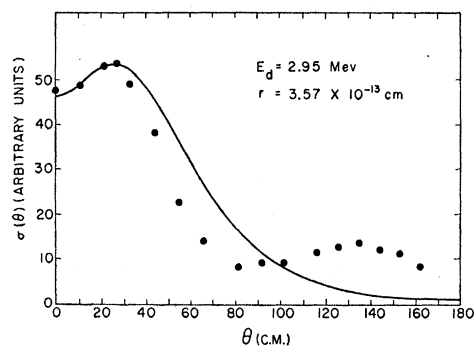
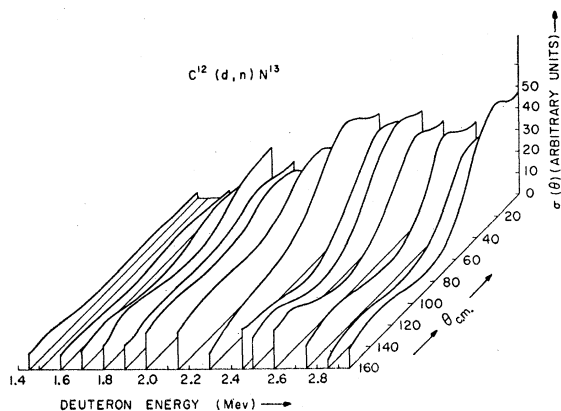


FIG. 13. Butler fit at 2.95 Mev.

that the heavy-particle stripping concept is not very helpful in understanding the backward peaking observed in this reaction. For comparison purposes Fig. 16 shows a plot of some of the cross sections as a function of the ordinary stripping momentum transfer vector  $q$ . (The factor  $\tau k_d^2$  is given in the tables of Lubitz<sup>19</sup> but is unimportant for the purposes of this discussion.) It can be seen that peaks are observed in the range  $q(10^{13} \text{ cm}^{-1}) = 0.20$  to  $0.26$  which are consistent with the conceptual nature of the radius parameter in ordinary stripping. Butler, Austern, and Pearson<sup>22</sup> suggest that surface reflection might be the mechanism responsible for the backward peaking. As explained earlier, the low  $Q$ -value of this reaction will favor simple stripping and we may anticipate that a fuller treatment of that process should explain the behavior in the backward as well as the forward hemisphere.

Further evidence for interference effects comes from the variation with deuteron energy of the stripping radius that gives the best fit in the simple theory. These radii are shown in Fig. 17; Fig. 17 shows their variation with deuteron energy. The interference effects distort the direct interaction pattern and this is reflected in the change of apparent stripping radius. Note in particular that in the region of  $E_d = 2.2$  Mev

FIG. 14. Over-all differential cross sections  $\sigma(E_d, \theta)$ .

<sup>22</sup> Butler, Austern, and Pearson, Phys. Rev. **112**, 1227 (1958).

where the total integrated cross section shows a broad maximum (Fig. 4), the ratio of  $0^\circ$  to  $180^\circ$  differential cross sections has a maximum value (approximate equality would be expected if a single true resonance dominated) and also the apparent stripping radius passes through a minimum.

It would be very valuable if we could subtract from our results the effects of compound nucleus formation and reveal the underlying direct interaction distribution for comparison with the detailed predictions of a more realistic model of the direct interaction. As we have emphasized, the interference effects that show up very clearly in our work make meaningless any simple subtraction procedure such as removing an "isotropic background" to represent compound nucleus formation. We might still advance tentatively in the following way.

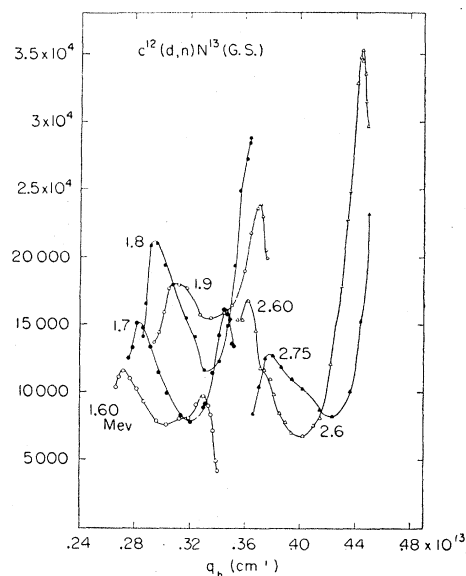


FIG. 15. Normalized yield, as a function of heavy-particle momentum transfer magnitude  $q_h$  for a number of bombarding energies. (Other values of the energy are omitted for clarity).

Even if compound nucleus formation is a minor contributor to the total cross section it will still, through its interference with the direct process, strongly affect the angular distribution; the processes are coherent. The interference terms themselves, however, will depend sharply on the bombarding deuteron energy since the phase of the compound nucleus contribution changes quickly by  $180^\circ$  as we pass across any one level while that of the direct process changes smoothly and slowly. If then we had angular distributions available at finely-spaced bombarding energies, they could be appropriately averaged over an energy range greater than the estimated level spacing in a manner that would remove the interference terms without determining them. In this way we could make the processes effectively incoherent. Our present results are numerous and enable us to make a first approxi-

mation of this plan without, however, having very great confidence in the outcome. We have chosen a procedure that enables us to allow to some degree for the expected change with bombarding energy of the direct interaction pattern itself.<sup>23</sup> We have seen that in the forward hemisphere the correspondence with the simple stripping pattern is good. We therefore, at each deuteron energy and for angles forward of  $90^\circ$ , refer our experimental results to our best fit to the simple stripping theory arbitrarily normalized at the peak of the angular distribution (see Figs. 8 through 13). These experimental to theoretical cross section ratios are then themselves suitably averaged and then used to reconstruct an average experimental cross section referred to a particular arbitrarily chosen deuteron energy (we have taken  $E_d = 2.85$  Mev). In the backward hemisphere we have no such theoretical pattern to guide us and so have simply averaged the experimental results, suitably fitted at  $90^\circ$  to those resulting from the earlier procedure in the forward hemisphere.

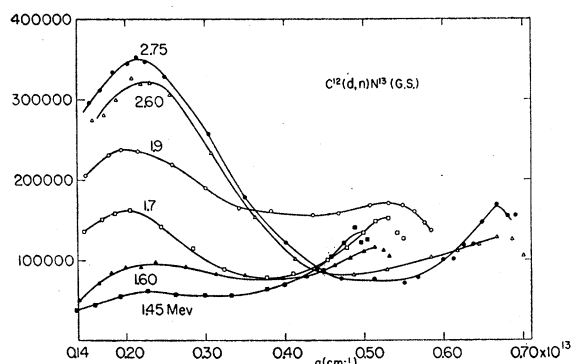


FIG. 16. Stripping momentum transfer. Normalized yield,  $N_{e.m.}(\theta)/\tau k d^2$ , as a function of the ordinary stripping momentum transfer magnitude  $q$  for a number of bombarding energies.

This is encouraged by the fact that the angle at which the backward maximum is found varies only very slightly and unsystematically with deuteron energy. The resultant averaged distribution is given in Fig. 18, together with the simple stripping pattern. We believe that to a crude approximation we have eliminated the direct interaction-compound nucleus interference terms and that what we have revealed is the direct interaction pattern plus a presumably more-or-less isotropic compound nucleus contribution. It seems that the latter term is probably quite small and perhaps very small. The closeness of the fit in the forward hemisphere between experiment and the simplest theory is astonishing. (In the averaging procedure we employed the fitted theoretical Butler angular distributions but we would like to emphasize

<sup>23</sup> The obvious way to introduce the effective incoherence is to use a target thick compared with the spacing between compound nucleus levels. This procedure is adequate, however, only if the direct interaction pattern itself is constant in this energy range.

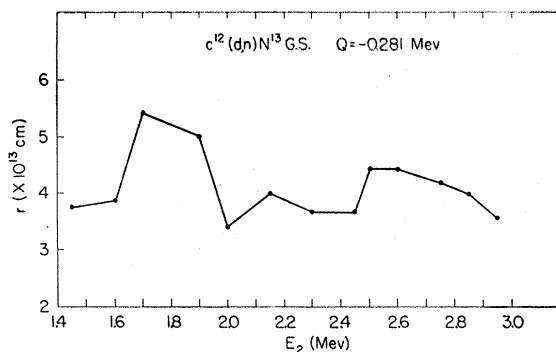


FIG. 17. Radius chosen for "best fit" to Butler theory as a function of deuteron bombarding energy.

that the described procedure is not essential to the method. Good agreement is obtained between experiment and the Butler theory even if other averaging processes are used [see Fig. 19].) We can offer no explanation for the excellent agreement between experiment and the simple theory until a realistic computation using distorted waves has been carried out. It will be of the greatest interest to see whether this calculation can account for the systematic behavior backwards of  $90^\circ$  for which the simple theory fails completely.

#### ACKNOWLEDGMENTS

This work was performed using the pulsed-beam system developed by Stuart Bloom and Clarence

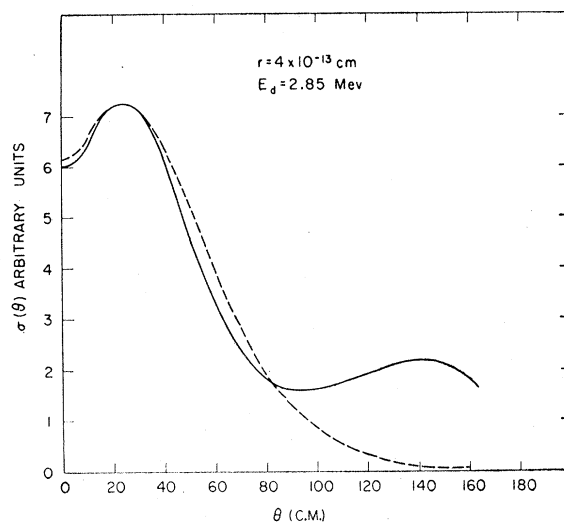


FIG. 18. Angular distribution (2.85 Mev,  $r=4$  fermis) with interferences removed. Dashed curve: Butler pattern for  $r=4.0 \times 10^{-13}$  cm and  $E_d=2.85$  Mev. Full curve: composite experimental curve for  $E_d=2.85$  Mev. (In the forward hemisphere at each  $E_d$  the experimental angular distribution has been expressed in terms of its best Butler fit for  $E_d \geq 1.9$  Mev. The logarithms of the ratios to Butler for all  $E_d$  at each angle have been added and their mean taken as a measure of departure from Butler averaged over the whole range of deuteron energies considered. In the backward direction the experimental results have been averaged and a fit made at  $90^\circ$ ).



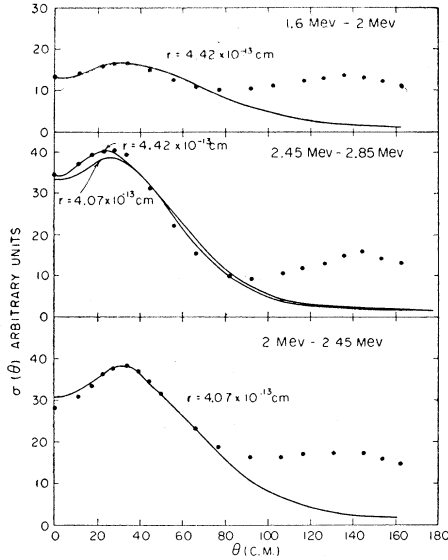


FIG. 19. Average of angular distributions in the regions of 1.6 Mev-2 Mev, 2 Mev-2.45 Mev, and 2.45 Mev-2.85 Mev. The dots in each of the 3 curves represent the arithmetic mean of the measured yields at each angle in the corresponding regions. Solid curves represent the Butler fits calculated for energies in the middle of the averaging regions.

Turner. This installation was an essential part of these measurements and the success of this device is gratefully acknowledged. In addition the authors are indebted to R. L. Chase and W. Higinbotham for their many helpful suggestions during the development of the millimicrosecond timing system used for these measurements.

We wish to thank R. Lindgren, E. Reilly, F. Rumph, C. Nawrocki, and A. Timpe for their efforts which speeded the progress of this work.

#### APPENDIX. EFFICIENCY OF THE PLASTIC DETECTOR

The detector is a cylinder of diameter  $h$  and length  $L$  uniformly irradiated by monoenergetic neutrons incident along its axis. The respective densities of hydrogen and carbon atoms are  $n_H$  and  $n_C$  and the respective nuclear neutron cross sections are  $\sigma_H$  and  $\sigma_C$ . Define  $\sigma_t = (n_H/n_C)\sigma_H + \sigma_C$ . The probability of a neutron interacting with hydrogen is

$$\frac{(n_H/n_C)\sigma_H}{\sigma_t} = \frac{\sigma_t - \sigma_C}{\sigma_t} = 1 - \frac{\sigma_C}{\sigma_t} = \lambda,$$

the fraction of incident neutrons that are absorbed is

$$1 - \exp[-(n_H\sigma_H + n_C\sigma_C)L] = 1 - \exp(-n_C\sigma_t L),$$

and the probability that the initial collision will be with a proton is

$$p_1 = \lambda[1 - \exp(-n_C\sigma_t L)].$$

Some of the neutrons scattered by carbon in the plastic will subsequently interact with a proton. The relative probability of an interaction with a carbon is

$$\frac{\sigma_C}{\sigma_t} = \frac{\sigma_t - (n_H/n_C)\sigma_H}{\sigma_t} = 1 - \lambda.$$

We call the probability that a neutron interacts with a proton after scattering from a carbon  $p_2$ .

Then the efficiency  $\epsilon$  is

$$\epsilon = p_1[1 + p_2(1 - \lambda) + p_2^2(1 - \lambda)^2 + \dots],$$

$$\epsilon = p_1/[1 - (1 - \lambda)p_2].$$

To calculate  $p_2$ , (a) we neglect the attenuation of the neutrons passing through the scintillator, (b) we assume that the carbon scattering is isotropic, and (c) we make the approximation that the neutron scattered from the carbon sees a spherical scintillator of the same volume as the cylinder, i.e.,

$$\frac{4}{3}\pi R^3 = \frac{1}{4}\pi h^2 L,$$

$$2R = \left(\frac{3}{2}h^2 L\right)^{1/3}.$$

The differential probability of a neutron seeing a length  $l$  of scintillator is

$$dp(l) = \frac{3}{4R} \left[ 1 - \left(\frac{l}{2R}\right)^2 \right] dl;$$

each of these lengths  $l$  has an absorption for neutrons given by

$$I(l) = 1 - \exp(n_C\sigma_t l),$$

so

$$p_2 = \int_0^{2R} I(l) dp(l).$$

Integration gives

$$p_2 = 1 - \frac{3}{2x} \left( 1 - \frac{2}{x^2} \right) - \frac{3}{x^2} e^{-x} \left( 1 + \frac{1}{x} \right)$$

where  $x = 2Rn_C\sigma_t$  or  $x = \left(\frac{3}{2}h^2 L\right)^{1/3} n_C\sigma_t$ .